

## Adsorption of Heavy Metal Ion from Aqueous Single Metal Solution by Aminated Epoxy-Lignin

Xinliang Liu, Hongxiang Zhu, Chengrong Qin, Jinghong Zhou, Joe R. Zhao, and Shuangfei Wang\*

This study investigated the adsorption of the heavy-metal ions Cu(II) and Pb(II) onto a lignin derivative. The lignin derivative was obtained by treating bagasse soda lignin with epichlorohydrin, and subsequently grafting an amine functional group by the Mannich reaction. The morphology of aminated epoxy-lignin was a layered structure with pores characterized by SEM. The heavy-metal ion adsorption data could be described well with the pseudo-first order model for Pb(II) ion and the pseudo-second order model for Cu(II) ion; diffusion was found to be the rate-limiting step when approaching equilibrium. FTIR spectroscopy was used to study the mechanism of heavy-metal adsorption by the derivatized lignin. The results show that the sites for adsorption are related to hydroxyl and amido groups.

*Keywords:* Mannich reaction; Lignin; Aminated lignin; Adsorption; Mechanism; Heavy metal

*Contact information:* College of Light Industry and Food Engineering, Guangxi University, Nanning 530004, P.R. China; \*Corresponding author: wangsf@gxu.edu.cn

### INTRODUCTION

As many industries have developed and expanded, water pollution has become a serious problem in the world, especially in the case of wastewater that contains heavy-metal ions, such as Cr, Zn, Pb, Cu, Ni, and Hg. For environmental remediation, many approaches and various kinds of cost-effective sorbents are used to remove heavy metal ions (Lee and Davis 2001; Sun *et al.* 2009; Wang and Chen 2009; Xu *et al.* 2012). Among those, biomass adsorbents are the most prominent materials since they are environmentally friendly and renewable.

Lignin has attracted scholar's attention, as it is one of the most abundant among various kinds of biomass waste. It is a pulping industrial by-product existing in black liquor, and more than  $50 \times 10^5$  tons of lignin are produced per year worldwide by pulping. However, less than 10% of this amount is utilized, and the rest is discharged; this is not only a waste of a natural resource, but also the cause of some serious environmental problems (Albadarin *et al.* 2011b).

The sorption behavior of black-liquor-derived lignin and its derivatives has been studied for the following ions Cu(II), Cr(III) (Wu *et al.* 2008), Cd(II) (Quintana *et al.* 2008), Ni(II), Zn(II), and Pb(II) (Demirbas 2004; Guo *et al.* 2008). Lignin adsorption capacity can be enhanced by chemical methods such as the addition of functional groups or cross-linking. In general, its adsorption capability has been attributed to the chemical functional groups, such as amino, carboxyl, hydroxyl, or phenolics (Demirbas 2007; Harmita *et al.* 2009).

The Mannich reaction is an important route to introduce primary or secondary amine groups (Mannich and Krösche 1912). Liu *et al.* (2011) obtained the aminated

lignin with a remarkably high uptake of Pb(II), up to 49.85 mg/g, by Mannich reaction. Lu *et al.* (2012) reported a maximum adsorption capacity of 60 mg/g for Cu(II) and 90 mg/g for Co(II) on copolymers prepared via Mannich reaction from lignin and amino acids. In addition, epoxidation is another modification of lignin (Malutan *et al.* 2008) that can improve the reactivity of lignin to amination.

In this paper, in order to obtain undissolved aminated lignin, the lignin was epoxidized with epichlorohydrin, and aminated *via* the Mannich reaction. The derivatized lignin was examined for its capabilities to remove Cu(II) and Pb(II) from aqueous solutions. The adsorption kinetics and mechanisms were investigated utilizing FTIR characterization.

## EXPERIMENTAL

### Materials

Lignin was isolated by acid precipitation from an industrial black liquor obtained from the soda pulping of bagasse (supplied by Nanning Sugar Industry Co., Ltd. China), and the isolated method was carried out as described by Nadji *et al.* (2010). The black liquor was filtered prior to acidulation in order to remove suspended solid residues. The filtered liquor was precipitated by acidification to pH 2 with sulphuric acid (40% w/w). The precipitation lignin was washed with 10% (w/w) sulphuric acid and distilled water. Then, the lignin was vacuum-dried in an oven at 70 °C.

All chemicals, including epichlorohydrin (from Tianjin Yongda Chemical Reagent Factory, China), diethylenetriamine, and formaldehyde (from Chendu Kelong Chemical Reagent Factory, China), were obtained from commercial sources. Aqueous solutions of Cu(II) and Pb(II) were prepared from copper chloride (from Tianjin Damao Chemical Reagent Factory, China) and lead nitrate (from Tianjin Yongda Chemical Reagent Factory, China) at a cation concentration of 300 mg/L; the initial pH of the solution was 5.52 for Cu(II) and 6.86 for Pb(II). All reagents were of analytical grade without being further purified. Distilled water was used to produce the metal ion solutions.

### Methods

#### *Preparation of aminated epoxy-lignin*

Epoxy lignin was produced by the method of Hu *et al.* (2007). Lignin (2 g) was added to 100 mL of 10% NaOH and 10 mL of 75% ethanol in a three-neck flask. To this mixture was added 10 mL of epichlorohydrin by use of a constant pressure funnel over 30 min. The mixture was stirred at 90 °C for 4 h. The product was then filtered and washed with benzene and distilled water and dried (at 50 °C) for further study and analysis.

Aminated epoxy-lignin was achieved by the Mannich reaction as described by Liu *et al.* (2005). Epoxy lignin (2 g), 15 mL of 10% NaOH, and 5 mL of diethylenetriamine were added into a 100 mL three-neck flask. Formaldehyde (5 mL) was added dropwise to the 80 °C heated mixture over 30 min. After the reaction proceeded for 3 h, the aminated epoxy-lignin was filtered and washed with distilled water and dried (at 70 °C) for further study and analysis.

### *Sorption experiments*

The metal ion adsorption experiments were performed in a conical flask with 200 mL of 300 mg/L Cu(II) or Pb(II) ion solution and 0.5 g aminated epoxy-lignin at room temperature (25 °C). The aqueous solutions were taken at preset time intervals, and the concentrations of ions were measured by the Atomic Absorption Spectrometer (TAS-990AFG). The amount of adsorption at time,  $t$ , was calculated by Equation (1),

$$q_t = \frac{V(C_0 - C_t)}{w} \quad (1)$$

where  $q_t$  is the adsorption capacity of adsorbent,  $V$  and  $w$  are the volume (L) of solution and the mass (g) of adsorbent, and  $C_0$  and  $C_t$  (mg/L) are the concentration of metal ions at time 0 and  $t$ , respectively.

The experiments of adsorption isotherm were processed in the ion solution at 200 mL of 50 mg/L, 100 mg/L, 150 mg/L, 200 mg/L, and 300 mg/L with 1 g of aminated epoxy-lignin.

### *Characterization*

The products were characterized by Fourier Transform Infrared spectroscopy (FTIR) using KBr pellets. FTIR spectra were recorded using a PerkinElmer BXII spectrum with the detector at  $4 \text{ cm}^{-1}$  resolution and 8 scans per sample from  $400$  to  $4000 \text{ cm}^{-1}$ . Scanning electron microscope (SEM) micrographs of the lignin and the aminated epoxy-lignin were recorded using Hitachi S-3400N to analyze the surface morphology changes.

## RESULTS AND DISCUSSION

### *SEM analysis*

SEM micrographs of the lignin and the aminated epoxy-lignin are displayed in Fig. 1. Comparing the surface morphology of lignin with that of aminated epoxy-lignin, it can be easily seen that changes occurred during the aminated and epoxidation processes. The underivatized lignin appeared granulated with grains of compact structure and different sizes, while the aminated epoxy-lignin appeared layered and porous.

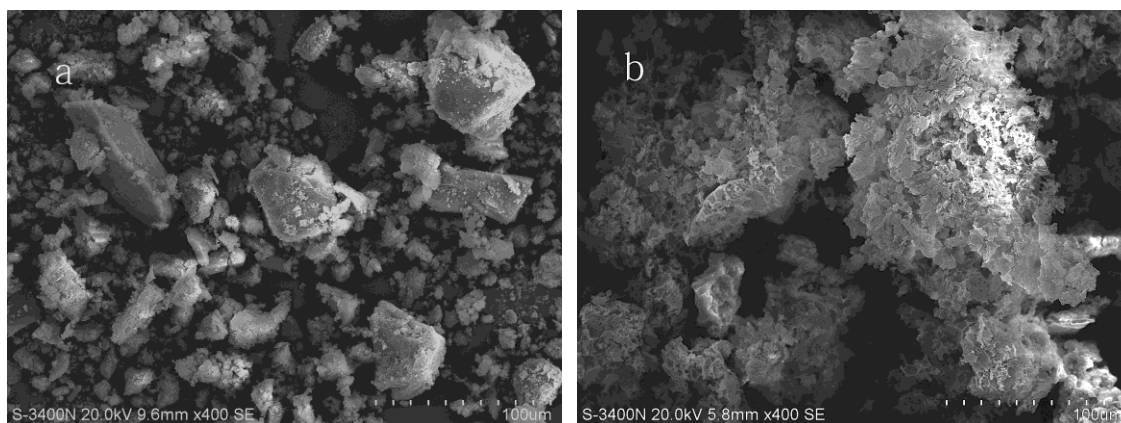


**Fig. 1.** Scanning electron microscopy image of lignin (a) and aminated epoxy-lignin (b)

These differences in appearance indicated that the lignin was dissolved and rebuilt in the course of the chemical treatment. The porous structure of aminated epoxy-lignin exhibited a large specific surface area, which presumably could increase the heavy-metal ion adsorption capacity of the material.

#### Fourier Transform Infrared spectrum analysis

To discuss the mechanism, the changes of function groups in lignin and its derivative were characterized by infrared spectroscopy in the near IR region (wave numbers 4000 to 500  $\text{cm}^{-1}$ ). A typical FTIR spectrum of lignin is shown in Fig. 2 (a). Corresponding results for the derivatized lignin are shown in Fig. 2 (b). Based on the assignments given by Singh *et al.* (2005), common features as well as particular vibrations, specific to each sample, were found in the spectra.

Various bands in the spectrum were identified as corresponding to O-H (at wavenumber of 3421  $\text{cm}^{-1}$ ), methoxyl (2848  $\text{cm}^{-1}$ ), aliphatic C-H (3000 to 2860  $\text{cm}^{-1}$ ), and aromatic C-H (3002  $\text{cm}^{-1}$ ) as well as aromatic skeletal (1426, 1514, and 1603  $\text{cm}^{-1}$ ). Absorption at 1463  $\text{cm}^{-1}$  relates to C-H deformations and aromatic ring vibrations. The aliphatic C-H stretching in  $\text{CH}_3$  and O-H in-plane bending gives a small band at 1361  $\text{cm}^{-1}$ . The bands at 1327, 1250, and 1227  $\text{cm}^{-1}$  are indicative of ring breathing with C-O stretching. The bands at 1127 and 1034  $\text{cm}^{-1}$  arise from the aromatic C-H in-plane deformation for syringyl type and guaiacyl type, respectively. Another band in the spectrum corresponded to lone aryl C-H wagging (834  $\text{cm}^{-1}$ ). The weak band at 617  $\text{cm}^{-1}$  is for the out-of-plane OH bending. The band at 2848  $\text{cm}^{-1}$  represented the symmetric  $\text{CH}_3$  stretch of the methoxyl group, and the band at 1034  $\text{cm}^{-1}$  was due to the C-O stretch for the O- $\text{CH}_3$  and C-OH.

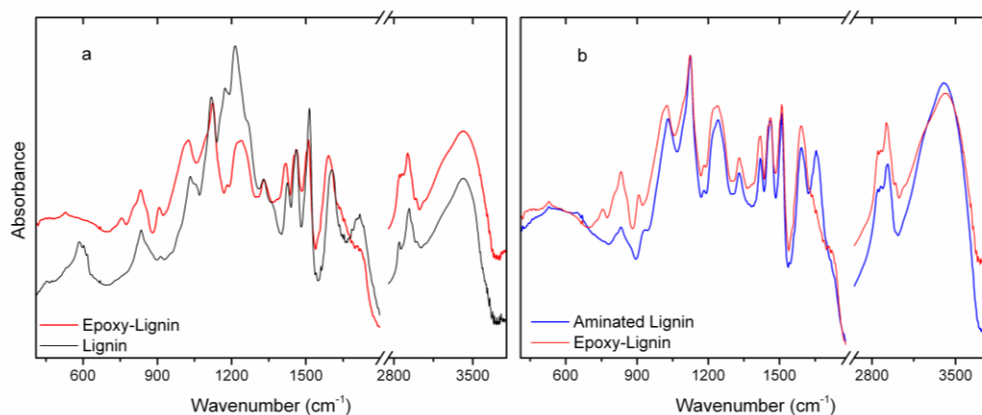


**Fig. 2.** IR spectrum (KBr) of Lignin before and after modification: (a) lignin before and after being cross-linked; (b) epoxy lignin before and after aminated

Comparing the starting lignin sample with the epoxy lignin, a pronounced change in the spectra was evident at 1718  $\text{cm}^{-1}$ . In Fig. 2 (a) this absorption corresponds to the C=O stretching of carbonyl and ester in conjunction with the aromatic ring. The shoulder peak at 1718  $\text{cm}^{-1}$  in the spectrum of epoxy lignin indicates that the ester decomposed and some carbonyl groups were present. The band at 1214  $\text{cm}^{-1}$ , which can be attributed to C-O stretching of phenolic OH and ether in syringyl and guaiacyl, showed a decrease, consistent with the reaction of phenolic OH in the process of etherification. In addition, the rising strong band at 1035  $\text{cm}^{-1}$  for the ether linkage (C-O-C) and the band appearing at 755  $\text{cm}^{-1}$  for 3-ring ether deformation suggest the grafting of epichlorohydrin onto the

lignin. Based on this, it can be inferred that the reaction of epichlorohydrin and lignin should occur on the phenolic hydroxyl.

Between the spectra of epoxy lignin and aminated epoxy-lignin, significant changes of the peaks were observed at 1654, 1025, 907, and 755  $\text{cm}^{-1}$  (Fig. 2b). A band at 1654  $\text{cm}^{-1}$  indicates the amide bond formed in aminated epoxy-lignin. The N-H stretching band merges with the hydroxyl peak (Müller *et al.*, 2009; Singh *et al.*, 2005), and C-N wagging band combines with the aromatic C-H bending peak. The C-N stretching may make the peak blue shift at 1025  $\text{cm}^{-1}$ . The phenolic C-H bending out of plane at 907  $\text{cm}^{-1}$  blue shifted to 935  $\text{cm}^{-1}$  could be considered to be a result of the electron cloud change of the benzene ring affected by the substituent. The peaks decrease at 1035  $\text{cm}^{-1}$  and disappear at 755  $\text{cm}^{-1}$ , confirming that the 3-ring ether was cleaved after amination. Thus, it can be concluded that the amination of lignin caused the cleavage of the 3-ring ether and changed the phenolic substituent.

### *Influence of solution initial pH*

The pH of a solution plays an important role in the adsorption of metal ions onto various adsorbents. In order to obtain the optimal pH for maximum removal efficiency, a sorption experiment was conducted in the initial pH range from 2 to 8 with the initial Cr(III) concentration of 300 mg/L, as shown in Fig. 3. By increasing the pH, the sorption capacities were reached for Pb(II) and Cu(II). At pH 4, about 50 mg/L Cu(II) and 45mg/L Pb(II) was adsorbed. Crist *et al.* observed that metal ion sorption was accompanied by stoichiometric release of protons and existing metals, and concluded that ion exchange mechanisms were responsible for the removal of metals by lignin (Crist *et al.*, 2002; Guo *et al.* 2008). When the pH was higher than 7, the precipitation of the metal ions occurred, resulting in a colloidal suspension. Thus, considering the precipitation of ions, the experimental pH was chosen to be in the range of 6 to 7.

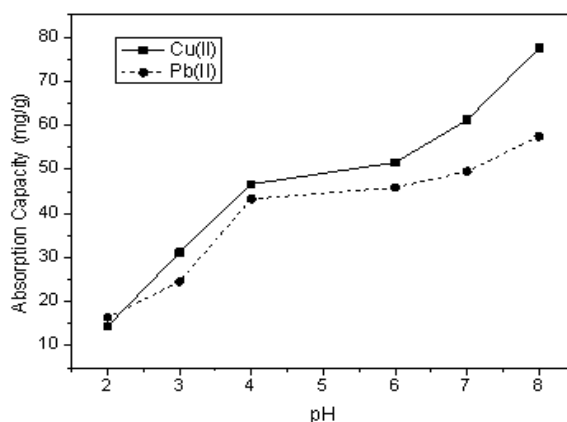


**Fig. 3.** The effect of initial pH (a) on adsorption

### *Isotherm models investigation*

Adsorption experimental data were fitted to the Langmuir and Freundlich isotherm models at various temperatures.

The Langmuir model is based on the monolayer adsorption of metal ions on the surface of sites of adsorbents, and the linear form can be expressed as (Hubbe *et al.* 2011; Karthikeyan *et al.* 2005),

$$\frac{C_e}{q_e} = \frac{1}{K_1 q} + \frac{C_e}{q} \quad (2)$$

where  $C_e$  (mg/L) and  $q_e$  (mg/g) are the concentration and amount adsorbed at equilibrium,  $q$  (mg/g) is the adsorption capacity, and  $K_1$  (L/mg) is a constant.

The Freundlich isotherm is an adsorption model suitable for multilayer adsorption, and its linear form can be expressed as (Hubbe *et al.* 2011),

$$\ln q_e = \ln b + K_2 \ln C_e \quad (3)$$

where  $b$  indicates the adsorption capacity (mg/g) and  $K_2$  is a parameter related to the intensity of adsorption.

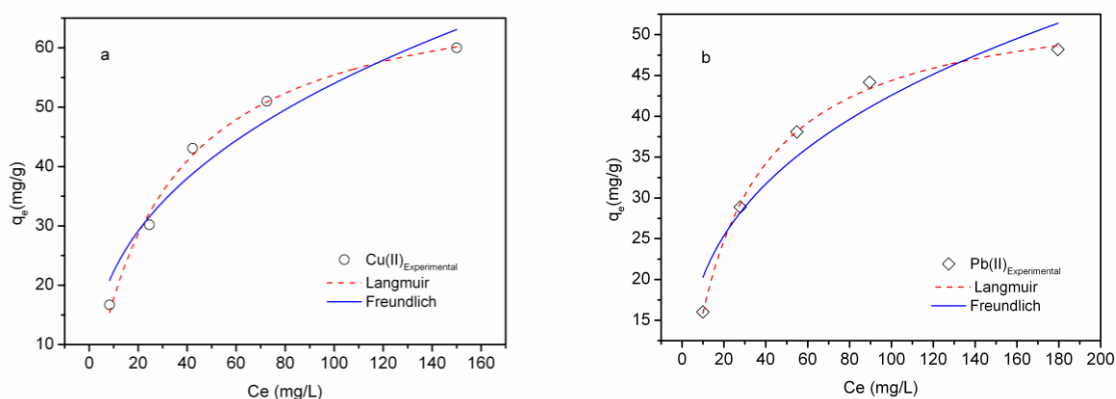


**Fig. 4.** Adsorption isotherms for Cu(II) (a) and Pb(II) (b) at 303 K

The theoretical parameters of isotherms along with regression coefficients are listed in Table 1. The isotherms are compared based on the parameter values with experimental data at 303 K, as shown in Fig. 4.

**Table 1.** Adsorption Isotherms of Cu(II) and Pb(II) onto Aminated Epoxy-Lignin at Different Temperatures

	$T$ (K)	Langmuir isotherm			Freundlich isotherm		
		$q$ (mg/L)	$K_1$ (L/mg)	$R^2$	$q$ (mg/L)	$K_2$	$R^2$
Cu(II)	303	72.48	0.0325	0.9920	9.24	0.3834	0.9348
	313	85.09	0.0399	0.9972	11.42	0.3885	0.9354
	323	97.60	0.0496	0.9914	14.03	0.3901	0.8972
Pb(II)	303	55.35	0.0404	0.9979	9.68	0.3217	0.9051
	313	66.69	0.0503	0.9961	12.33	0.3227	0.9056
	323	77.89	0.0645	0.9985	15.36	0.3232	0.8912

Based on results given in Table 1, the Langmuir isotherm model was found to have a good fit with the experimental data ( $R^2 > 0.99$ ). The maximum adsorption capacity ( $q_{max}$ ) obtained from the Langmuir isotherm model was 72.48 mg/g for Cu(II) and 55.35

mg/g for Pb(II). For the Freundlich isotherm model,  $K_2$  values were in the range  $0.1 < K_2 < 1$ , indicating that the adsorptions of Cu(II) and Pb(II) were favorable (Hubbe *et al.* 2011). The results also suggested that the bond energies increased with increasing surface density.

#### Thermodynamic investigation

Thermodynamic parameters were calculated as indicated by Albadarin *et al.* (2011b). The values of  $\Delta H^\circ$ ,  $\Delta S^\circ$ ,  $\Delta G^\circ$ , and  $E_a$  for the adsorption of Cu(II) and Pb(II) on the aminated epoxy-lignin are listed in Table 2. The  $\Delta H^\circ$  value obtained indicated that the adsorption process was endothermic in nature. The value of  $\Delta S^\circ$  obtained reflects the increased randomness at the solid/solution interface during the adsorption process. The values of  $\Delta G^\circ$  indicate that it is spontaneous for the adsorption of Cu(II) and Pb(II) within the range of temperature being studied. The decrease in the  $\Delta G^\circ$  values with temperature suggests that the process is feasible at higher temperatures.

**Table 2.** Thermodynamic Parameters for the Adsorption of Cu(II) and Pb(II) onto Aminated Epoxy-Lignin

$\Delta H$ (kJ/mol)	$\Delta S$ (J/mol K)	$E_a$ (kJ/mol)	$\Delta G$ (kJ/mol)		
			303K	313K	323K
19.01	225.41	17.19	-49.29	-50.54	-53.79
14.58	217.59	19.01	-41.35	-53.52	-55.7

#### Adsorption kinetics investigation

The kinetics of adsorption describes the rate of adsorbate uptake and the time taken to achieve equilibrium. The rates of Cu(II) and Pb(II) sorption were studied at an initial ion concentration of 300 mg/L and a lignin dose of 0.5 g, in a conical flask on a mechanical shaker. As shown in Fig. 5, the kinetic data indicate that the initial adsorption rate was high during the first 30 min, and the amount of Cu(II) and Pb(II) adsorbed was 67.76 mg/g and 49.64 mg/g, respectively. The pH decreased to 4.86 and 3.48, respectively, for each heavy-metal ion adsorbed. The adsorption capability of aminated epoxy-lignin can be attributed to the active function groups on the surface, such as amine, hydroxyl, and carboxyl groups (Albadarin *et al.* 2011a). At the initial stage, a higher number of sites was available for the trapping of metal ions. The hydrogen ion in the carbonyl group or amine group present in lignin was subject to displacement by ion exchange. This made the pH decrease rapidly during the initial stages. After the sites had been occupied by the cations, the surface of the adsorbent became exhausted and the adsorption rate was limited by the transport of ions from the outer sites to the interior sites. This can be attributed to the driving force for adsorption, as is assumed when applying the pseudo-first order and pseudo-second order models. These two models can be expressed as Equations (2) and (3), respectively (Albadarin *et al.* 2011a):

$$q = q_e(1 - e^{-k_1 t}) \quad (4)$$

$$q = \frac{q_e^2 k_2 t}{1 + q_e k_2 t} \quad (5)$$

where  $q_e$  and  $q$  (mg/g) are the amounts of adsorbent adsorbed at equilibrium and at any time,  $t$  (min.);  $k_1$  (1/min) and  $k_2$  (g/(mg•min)) are the adsorption rate constants of the pseudo-first order model and the pseudo-second order model, respectively.

The values of the rate constant for the pseudo-first order model and pseudo-second order kinetic model were obtained from the plots fitted by ORINGINPRO 8.6 software and are given in Table 3. The table shows that the pseudo-first order model was better for Cu(II) adsorption, and the pseudo-second order model was better for Pb(II) adsorption. The outermost electron shell of Cu(II) more easily accepts electrons of the coordinating group. Thus the reactions of the adsorption process would be as indicated in Equations (4) and (5):



where  $A$  represents the polar sites on the adsorbents.

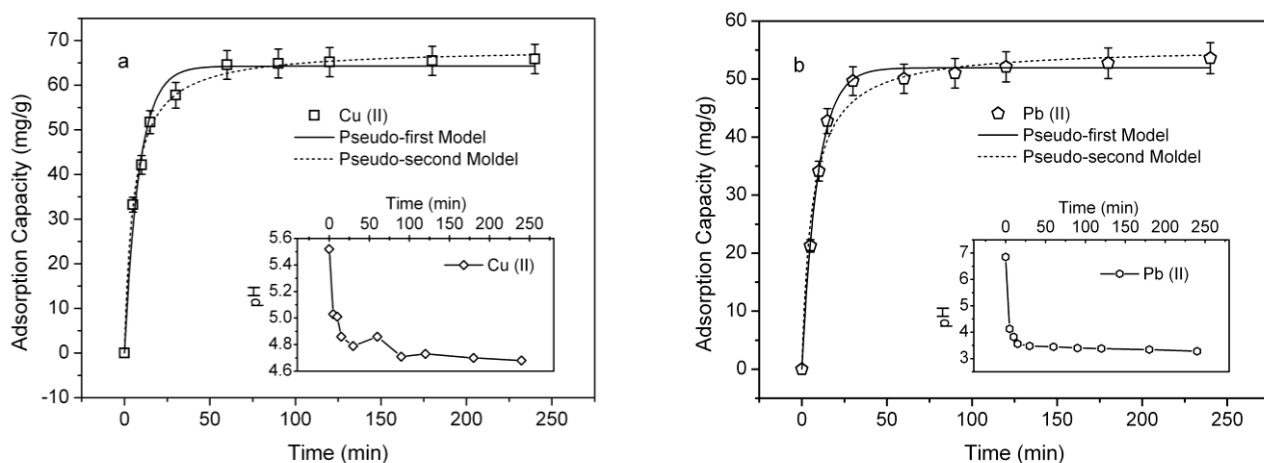


**Fig. 5.** Kinetics model for Cu(II) (a) and Pb(II) (b) adsorbed onto aminated epoxy-lignin at room temperature (25 °C).

The intra-particle diffusion model was of major concern because it is the rate-determining step in the liquid adsorption system. In order to investigate the diffusion mechanism within the adsorption system, intra-particle diffusion models were employed. A Webber's pore diffusion model (Ho and McKay 1998) was applied to the kinetic data for the pore diffusion factor as described by Equation (8),

$$q = k_{diff} t^{1/2} \quad (8)$$

where  $k_{diff}$  is the intra-particle diffusion rate constant (mg/(g•min.<sup>0.5</sup>)) determined from the slope of the plot of  $q$  versus  $t^{0.5}$ . If intra-particle diffusion was the rate limiting step, then this plot will be linear with the slope being  $k_{diff}$  and the  $y$ -intercept passing through the origin at  $t = 0$ .

**Table 3.** Pseudo-First Order Model and Pseudo-Second Order Model for the Adsorption of Cu(II) and Pb(II)

Kinetic Models and Parameters	$q_{e,exp}$ (mg·g <sup>-1</sup> )	Pseudo-First Order Model			Pseudo-Second Order Model		
		$q_e$ (mg·g <sup>-1</sup> )	$K_1$ (min <sup>-1</sup> )	$R^2$	$q_e$ (mg·g <sup>-1</sup> )	$K_2$ (g·mg <sup>-1</sup> ·min <sup>-1</sup> )	$R^2$
Cu(II)	67.76	64.2834	0.1161	0.9845	68.3307	0.00271	0.9965
Pb(II)	49.61	51.9284	0.1086	0.9964	55.5064	0.00295	0.9838

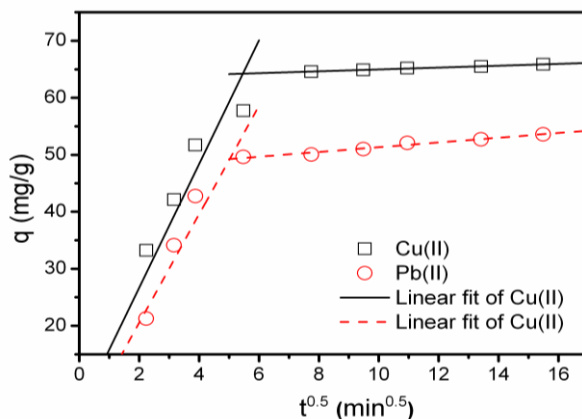
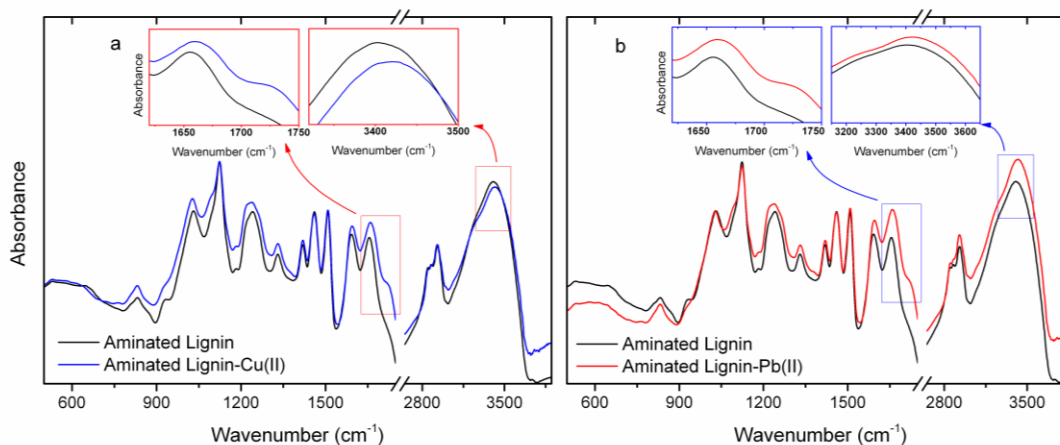
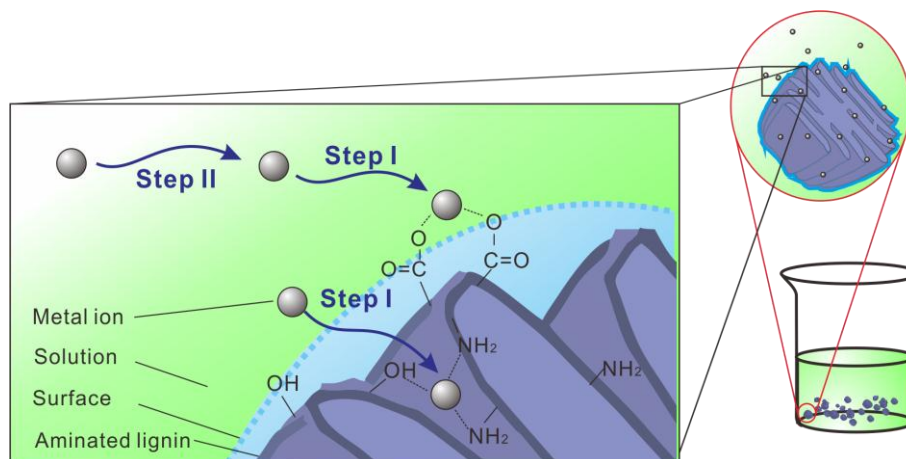
**Fig. 6.** Diffusion model for Cu(II) and Pb(II) adsorbed onto aminated epoxy-lignin at starting pH 6 and room temperature 25 °C

Figure 6 shows that the adsorption process consisted of two steps and the linearization did not pass through the origin. This indicates that the intra-particle diffusion was not the rate-limiting step and implies that the biosorption was affected by more than one process. The initial part of the plots suggests external mass transfer by film diffusion, and the latter part of the plots suggests intra-particle or pore diffusion, according to Albadarin *et al.* (2011a).

**Fig. 7.** IR spectrum (KBr) of Lignin before and after modification: (a) epoxy-lignin-amine before and after Cu (II) adsorption; (b) epoxy-lignin-amine before and after Pb (II) adsorption

### Mechanism of adsorption

Comparing the FTIR spectra for lignin before and after adsorption, based on differences of the vibrational parameters (frequency, band shape, and relative intensity), the possible interactions with the metallic ions were considered (Pereira *et al.*, 2007). The main changes observed were the increase of the relative intensities of the bands at 1603 and 1654  $\text{cm}^{-1}$ , which was assigned to C=C aromatic ring stretching and to C-N stretching, respectively. The spectral changes observed were due to the presence of the metallic ions interacting with the aminated lignin. Other obvious changes of the spectra before and after Cu(II) adsorption occurred at 3402, 1330, 1241, 1030, and 832  $\text{cm}^{-1}$  wavelengths, as shown in Figs. 7 (a) and (b). The peaks of the aromatic hydroxyl band arising at 1330  $\text{cm}^{-1}$  and broadening at 1241  $\text{cm}^{-1}$  suggest that the hydroxyl or amido groups may share its unpaired electrons with the metal ions (Harmita *et al.* 2009). The aromatic ring stretching is affected by the  $\pi$ -electron cloud moving with the bands arising at wavelengths of 1603  $\text{cm}^{-1}$  and 832  $\text{cm}^{-1}$ . The shoulder peak was strengthened at 1718  $\text{cm}^{-1}$ , which indicates the carbonyl groups could have interacted with the heavy-metal ions and caused the pH to decrease, as shown in Fig. 5. The C-N and N-H stretching changes resulted in the 1030  $\text{cm}^{-1}$  peak and in red shift of the peak at 3402  $\text{cm}^{-1}$ ; this observation conforms to the inferences of the amino group band at 1654  $\text{cm}^{-1}$ . However, there were some noticeable differences for lead adsorption in the regions 3401, 1030, and 400 to 600  $\text{cm}^{-1}$ , which can be contributed from the different electron distribution of copper and lead ions. Based on the interpretation of the FTIR spectra data along with the previous kinetic data, the following mechanism of heavy-metal ion adsorption was proposed, as depicted in Fig. 8:



**Fig. 8.** Proposed mechanisms for copper adsorption on aminated epoxy-lignin

According to this mechanism, metal ion adsorption by aminated epoxy-lignin occurs in two steps: the first is adsorption of metal ions onto the outer and inner binding sites; concentration differences are then generated between the solution near and far from the adsorbents' surface, forcing the metal ions to diffuse towards the adsorbents. Based on the kinetic studies, at the initial stage, the adsorption process is controlled by the surface complexation of the cations. Afterwards, intra-particle diffusion limits the heavy-metal ion adsorption by the modified lignin as the system approaches equilibrium. According to (Da'na and Sayari 2011) and Parajuli *et al.* (2006), the adsorption of metal ions onto lignin would involve ion exchange and complexation.

## CONCLUSIONS

With petroleum resources becoming depleted, bioresources are approaching a point of breakthrough in the field of polymeric materials. The conversion and utilization of bioresources are the primary problems. In this study, lignin, which has been considered as a waste product of the pulping industry, was modified to improve its adsorption capability for metal ions. Based on the present work it can be concluded that:

1. The surface morphology of aminated epoxy-lignin has a layered, porous structure, as characterized by SEM.
2. The adsorption kinetic data could be fit well by the pseudo-first order model and the pseudo-second order model for Pb(II) and Cu(II) ions, respectively; diffusion was the rate-limiting step for adsorption when approaching equilibrium. Adsorption capacities conformed well to a Langmuir model.
3. In addition, based on the FTIR spectra analyses, it was confirmed that the adsorption sites on the derivatized lignin are related to hydroxyl and amido groups.

## ACKNOWLEDGMENTS

This work was financially supported by the National High Technology Research and Development Program (863 Program) (2009AA06A416 & 2010GXNSFE 013006), National Water Special Research Program (2008ZX07317-02-03A2), Innovation Project of Guangxi Graduate Education (GXU11T31079), and Research Funds of the Guangxi Key Laboratory of Environmental Engineering (0804K016).

## REFERENCES CITED

- Albadarin, A. B., Al-Muhtaseb, A. A. H., Al-laqtah, N. A., Walker, G. M., Allen, S. J., and Ahmad, M. N. M. (2011a). "Biosorption of toxic chromium from aqueous phase by lignin: Mechanism, effect of other metal ions and salts," *Chemical Engineering Journal* 169(1-3), 20-30.
- Albadarin, A. B., Al-Muhtaseb, A. A. H., Walker, G. M., Allen, S. J., and Ahmad, M. N. M. (2011b). "Retention of toxic chromium from aqueous phase by H<sub>3</sub>PO<sub>4</sub>-activated lignin: Effect of salts and desorption studies," *Desalination* 274(1-3), 64-73.
- Crist, R. H., Martin, J. R., and Crist, D. R. (2002). "Heavy metal uptake by lignin: Comparison of biotic ligand models with an ion-exchange process," *Environmental Science and Technology* 36(7), 1485-1490.
- Da'na, E., and Sayari, A. (2011). "Optimization of copper removal efficiency by adsorption on amine-modified SBA-15: Experimental design methodology," *Chemical Engineering Journal* 167(1), 91-98.
- Demirbas, A. (2007). "Adsorption of Co(II) and Hg(II) from water and wastewater onto modified lignin," *Energy Sources Part a-Recovery Utilization and Environmental Effects* 29(2), 117-123.

- Demirbas, A. (2004). "Adsorption of lead and cadmium ions in aqueous solutions onto modified lignin from alkali glycerol delignification," *Journal of Hazardous Materials*, 109(1-3), 221-226.
- Guo, X., Zhang, S., and Shan, X.-Q. (2008). "Adsorption of metal ions on lignin," *Journal of Hazardous Materials* 151(1), 134-142.
- Harmita, H., Karthikeyan, K. G., and Pan, X. (2009). "Copper and cadmium sorption onto kraft and organosolv lignins," *Bioresource Technology* 100(24), 6183-6191.
- Ho, Y., and McKay, G. (1998). "Kinetic models for the sorption of dye from aqueous solution by wood," *Trans. IChemE* 76, 183-191.
- Hu, C., Fang, G., Wang, X., and Li, J. (2007). "Synthesis of straw alkaline lignin-based epoxy resin," *Journal of North-East Forestry University* 35(4), 53-55.
- Hubbe, M. A., Hasan, S. H., and Ducoste, J. J. (2011). "Cellulosic substrates for removal of pollutants from aqueous systems: A review. 1. Metals," *BioResources* 6(2), 2161-2914.
- Karthikeyan, T., Rajgopal, S., and Miranda, L. R. (2005). "Chromium(VI) adsorption from aqueous solution by *Hevea brasiliensis* sawdust activated carbon," *Journal of Hazardous Materials* 124(1-3), 192-199.
- Lee, S. M., and Davis, A. P. (2001). "Removal of Cu(II) and Cd(II) from aqueous solution by seafood processing waste sludge," *Water Research* 35(2), 534-540.
- Liu, Z., Chen, Z., and Wang, D. (2005). "Preparation and characterization diethylenetriamine/formaldehyde modified lignin amine," *Transaction of China Pulp and Paper* 20(2), 75-79.
- Liu, Z., Lv, S., Yan, X., Zhang, T., and Zeng, W. (2011). "Adsorption of lead ions in effluent onto lignin amines adsorbents from modified kraft lignin," *Transaction of China Pulp and Paper* 26(2), 53-57.
- Lu, Q.-F., Huang, Z.-K., Liu, B., and Cheng, X. (2012). "Preparation and heavy metal ions biosorption of graft copolymers from enzymatic hydrolysis lignin and amino acids," *Bioresource Technology* 104 (January), 111-118.
- Müller, G., Schöpfer, C., Vos, H., Kharazipour, A., and Polle, A. (2009). "FTIR-ATR spectroscopic analysis of changes in wood properties during particle-and fibreboard production of hard-and softwood trees," *BioResources* 4, 49-71.
- Malutan, T., Nicu, R., and Popa, V. I. (2008). "Lignin modification by epoxidation," *BioResources* 3(4), 1371-1376.
- Mannich, C., and Krösche, W. (1912). "Ueber ein Kondensationsprodukt aus Formaldehyd, Ammoniak und Antipyrin," *Archiv der Pharmazie* 250(1), 647-667.
- Nadji, H., Bedard, Y., Benaboura, A., Rodrigue, D., Stevanovic, T., and Riedl, B. (2010). "Value-added derivatives of soda lignin from alfa grass (*Stipa tenacissima*). I. Modification and characterization," *Journal of Applied Polymer Science* 115(3), 1546-1554.
- Parajuli, D., Kawakita, H., Inoue, K., and Funaoka, M. (2006). "Recovery of gold(III), palladium(II), and platinum(IV) by aminated lignin derivatives," *Industrial and Engineering Chemistry Research* 45(19), 6405-6412.
- Pereira, A. A., Martins, G. F., Antunes, P. A., Conrado, R., Pasquini, D., Job, A. E., Curvelo, A. A. S., Ferreira, M., Riul, A., Jr., and Constantino, C. J. L. (2007). "Lignin from sugar cane bagasse: Extraction, fabrication of nanostructured films, and application," *Langmuir* 23(12), 6652-6659.

- Quintana, G. C., Rocha, G. J. M., Goncalves, A. R., and Velasquez, J. A. (2008). "Evaluation of heavy metal removal by oxidised lignins in acid media from various sources," *BioResources*, 3(4), 1092-1102.
- Singh, R., Singh, S., Trimukhe, K. D., Pandare, K. V., Bastawade, K. B., Gokhale, D. V., and Varma, A. J. (2005). "Lignin-carbohydrate complexes from sugarcane bagasse: Preparation, purification, and characterization," *Carbohydrate Polymers* 62(1), 57-66.
- Sun, B., Mi, Z.-T., An, G., Liu, G., and Zou, J.-J. (2009). "Preparation of biomimetic materials made from polyaspartyl polymer and chitosan for heavy-metal removal," *Industrial and Engineering Chemistry Research* 48(22), 9823-9829.
- Wang, J., and Chen, C. (2009). "Biosorbents for heavy metals removal and their future," *Biotechnology Advances*, 27(2), 195-226.
- Wu, Y., Zhang, S., Guo, X., and Huang, H. (2008). "Adsorption of chromium (III) on lignin," *Bioresource Technology* 99(16), 7709-7715.
- Xu, L., Wang, J. N., Meng, Y., and Li, A. M. (2012). "Fast removal of heavy metal ions and phytic acids from water using new modified chelating fiber," *Chinese Chemical Letters* 23(1), 105-108.

Article submitted: September 5, 2012; Peer review completed: October 25, 2012; Revised version received: February 21, 2013; Accepted: February 23, 2013; Published: March 14, 2013.